Silicon (2019) 11:339–344
https://doi.org/10.1007/s12633-018-9869-1

ORIGINAL PAPER

Esterification of 1-Octanol on Clinoptilolite-Supported TiO_2 Catalysts

Bensu Özyağcı[1] · **Volkan Şahin**[2] · **Abdulkerim Karabakan**[2]

Received: 30 January 2018 / Accepted: 5 April 2018 / Published online: 5 June 2018

Abstract

In this study, a natural type of zeolite, Clinoptilolite (CLI), is used as a support for TiO_2. First, TiO_2-supported heterogeneous catalysts originated from the high temperature calcination of $TiCl_4$ groups, which were thermally immobilized on clinoptilolite, were obtained. Powder-XRD and EDX analyzes showed that the oxide form of Ti-immobilized on dealuminated clinoptilolite were formed in the anatase phase, and the zeolite structure was preserved. As seen in TGA/DTA analyzes, this catalyst could be efficient and have high stability for many reactions. Second, the esterification reaction of 1-octanol with acetic acid is used as a reference reaction for this catalyst.

Keywords Zeolite · Clinoptilolite · Titanium dioxide · Catalysis · Esterification · Octanol

1 Introduction

A natural type of zeolite, Clinoptilolite, which originates from Bigadiç/Turkey, has a big potential to be used as supports for heterogeneous catalysts for several industrial and environmental applications owing to the porous structure and high ion-exchange capability [1–5]. Titanium dioxide can be considered as an appropriate material by its cheapness and its stability toward chemical and photochemical corrosion. TiO_2 has the energies of $+3.1$ and -0.1 V for valence (VB) and conductivity (CB) bands respectively, and has a band gap of 3.2 eV. With the absorption of the photons in the UV range ($\lambda < 387$ nm), electron/hole pairs (exciton) are formed between the valence and conductivity bands. e^-/h^+ pairs and oxidant species can interact to form radicalic species, which can lead to the oxidation of the organic molecules [6, 7].

Titanium dioxide has been seen as an appropriate material for several applications thanks to its chemical and photochemical stability and cheapness. They can be used as fine powder or in crystal form, however, separation processes are very challenging and expensive, especially for environmental applications. For this purpose, fiberglass [8–10], silica [7, 11], and zeolites [9, 12] were used as supports for immobilizing TiO_2. Among these support materials, zeolites have attracted more attention than other support materials because they possessed ordered and unique pore and channel structures. According to a previous study, it has been observed that the use of zeolite as a support material for the immobilization of TiO_2, does not change the activity of TiO_2 or the adsorption properties of zeolites [13].

TiO_2 is found in many forms as mainly anatase, rutile and brookite, of which anatase has a low thermal stability and transforms into rutile when heated to 400–500 °C. Also the transformation to rutile increases with temperature [14]. In order to stabilize anatase phase at higher temperatures is an important key point for TiO_2 applications [15–17].

Organic esters can be produced by using several synthetic methods, generally with a carboxylic acid and an alcohol with the presence of an acid catalyst. This reaction takes place very slowly when there is no strong acid present [18]. One of the main components of the essential oils derived from fruits is octyl acetate, which is also used in food industry as aroma, odor component in perfumes and to prevent the bitter taste of the alkaloids. 1-octyl acetate is obtained from 1-octanol and acetic acid. In this study, clinoptilolite-supported TiO_2 catalysts were synthesized in order to investigate the catalytic esterification of N-octanol.

There is a limited amount of studies for the synthesis of octyl acetate. Balakrishnan et al. have used polymer-

---

Electronic supplementary material The online version of this article (https://doi.org/10.1007/s12633-018-9869-1) contains supplementary material, which is available to authorized users.

✉ Abdulkerim Karabakan
kerimk@hacettepe.edu.tr

[1] Department of Chemistry, İzmir Institute of Technology, İzmir 35433, Turkey

[2] Department of Chemistry, Hacettepe University, Ankara 06800, Turkey

supported $TiCl_4$ catalysts to investigate the reaction kinetics of n-octanol and acetic acid esterification reaction. The reaction order was found to be pseudo first-order and the activation energy was found to be 58.8 kJ/mol [19]. The same reaction was used by Choudary et al. with Cu^{2+} immobilized Montmorillonite catalysts. For the reaction (1:10 octanol/HOAc) at 389 K, 98% yield was obtained, according to the H-NMR data [20]. Izumi et al. used $H_3PW_{12}O_4$ containing silica as a catalyst for the esterification of several alcohols in between the reaction temperatures of 40–100 °C [21]. As a result, it is found that the reaction is a second-order reaction and at 80 °C, the ester yield is found to be 47%. As the carbon chain of the reactant alcohol increases, the hydrophobicity of the alcohol increases. The heteropoly acid-immobilized silica has hydrophilic acid sites, so it is difficult for alcohols to interact with the acid sites. Besides these studies, Amberlyst-36 [22], and $H_3PW_{12}O_4$ immobilized MCM-41 [23] were used as catalyst for this esterification reaction. To the best of our knowledge, there is no report dealing with a clinoptilolite-supported TiO_2 catalyst used for esterification reactions of alcohols with acetic acid as a heterogeneous catalyst.

2 Experimental

All pure analytical reagents were purchased from commercial sources. The preparation of catalyst and the catalytic reactions were carried out in a batch reactor placed in a Teflon heater and equipped with a reflux condenser and a magnetic stirrer.

2.1 Dealumination of Clinoptilolite

Bulk clinoptilolite (CLI) was treated with HCl for dealumination. 1 M HCl solution is used for a specific amount of zeolite, in which the mixture were refluxed at 100 °C for 6 h. At the end of the reaction, dealuminated zeolite were filtered and washed with distilled water, then dried overnight at 80 °C.

2.2 TiO_2 Formation on Dealuminated Clinoptilolite

2.0 ml HCl and 10.0 g deAl-CLI were mixed in 300 ml of distilled water. The theoretical loading amount were accepted as 30% (w/w), and 0.455 M $TiCl_4$ were added to the suspension. The pH of the solution was adjusted to 6 by aqueous $NH_3.H_2O$, then the hydrolysis reaction were conducted at 40 °C for 1 h. Later, the white suspension formed was filtered, washed and dried at 105 °C at 10 h. The dry product was calcinated at 700 °C in dynamic atmosphere for 2 h.

2.3 Esterification of 1-Octanol with Acetic Acid

6 mmol 1-octanol, 0.100 g TiO_2-CLI and 24 mmol HOAc were put into a round flask and the mixture were refluxed between the temperatures 100–140 °C for 3 h. At the end of the reaction the product mixture were filtered in order to separate the catalyst. The product was initially purified from the reactants by using column chromatography (EtOAc:Hex, 1:4) and 10 μL of samples were dissolved in 1 ml of CH_2Cl_2, in order to confirm the esterification reaction by using GC-MS analysis.

2.4 Characterization of the Samples

Adsorption isotherms of nitrogen were carried on a Quadrasorb SI Automated Surface Area and Pore Size Analyzer apparatus following the BET procedure. The IR spectra of the KBr pellets of the raw and modified zeolites were characterized using a Perkin Elmer precisely Spectrum One FT-IR spectrometer in the range of 4000–450 cm^{-1}. Powder X-ray diffraction patterns of the samples were recorded on a Rigaku D/Max 2200 PC diffractometer using Cu K_α radiation (λ = 1.54056 Å). The diagrams were recorded in the 2–50 (2h) range at a scan speed of 2 min^{-1} and a time constant of 1 s. The catalyst specimens were classified according to recognized zeolitic types from the diffractograms obtained. Thermal analysis of the samples was performed on a Shimadzu DTG-60H Simultaneous DTA-TG apparatus from 303 to 1173 K with a heating rate of 10 K min^{-1}. GC-MS analyzes were performed by using Agilent 6890 GC-Restek RTX, 30 m column and with Agilent 5973 mass analyzer. EDX analyzes were performed by using Oxford Instruments X-Supreme 8000 EDXRF spectrometer with a 5 keV energy.

3 Results and Discussion

The crystal structure of TiO_2 catalysts formed on clinoptilolite were identified by Powder X-ray diffraction method. Pure TiO_2 diffractions can be seen in Fig. 1. The unit cell parameters for anatase TiO_2 is a = 3.784 Å, c = 9.514 Å (Tetrahedral, I41/amd space group) [24]. The diffraction pattern matches with the reference unit cell parameters.

There is no diffraction signal could be attributed to the crystalline Ti catalyst in the X-ray diffraction of the calcined sample at 400 °C after the hydrothermal reaction. There are weak signals that belongs to the deAl-CLI crystals laminated with amorphous $TiCl_4$ on its surface. For the case of increasing the calcination temperature to 500 °C, nearly disappearing the zeolitic signals and the weak diffraction simultaneously arising signal at d-spacing = 3.53 Å indicates that the TiO_2 crystallization started at

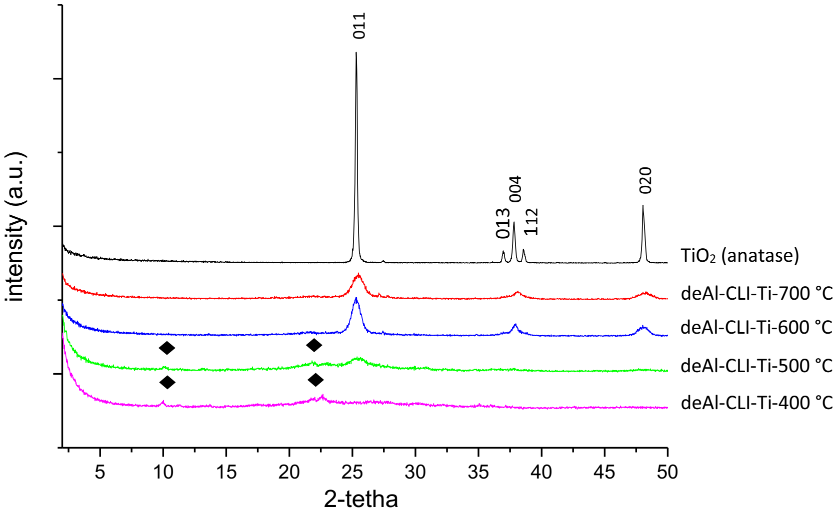

Fig. 1 Powder-XRD diffractograms of the catalysts; TiO_2 at anatase crystal phase (black/top), deAl-Al-CLI-Ti calcinated at 700 °C (red), calcinated at 600 °C (blue), calcinated at 500 °C (green), calcinated at 400 °C (magenta/bottom). Diffraction signals acquired on the product was calcinated at 700 °C, they have shifted to smaller d-spacings and become more broadened. ♦: Signals originating from CLI zeolite

this temperature. The supported deAl-CLI-Ti catalyst which was calcinated at 600 °C shows the signals clearly at the same d-spacing values for the anatase crystal structure of TiO_2 (Fig. 1). As the result of calcination at 700 °C unit cell parameters of TiO_2 crystals in the anatase structure have slightly deviated from the expected, with all the diffraction signals shifting to smaller d-spacings and becoming more broadened. The broadening of the diffraction signals for supported TiO_2 catalyst indicates the decrease in the catalyst size or formation of thin layers on CLI surface. A different atomic layer desorption (ALD) thin film crystal growth for $TiCl_4$ with surface -OH groups at 600 °C, than at aqueous media in which lower temperature and pressure, is known [25]. Hydrothermal synthesis method was established in order to make the titanium atoms originating from $TiCl_4$ is equal to the 30% of the CLI used. As the anatase TiO_2 crystals covered the support's surface effectively, no signals for CLI zeolite crystals were observed. For the deAl-CLI-Ti supported catalyst, the surface area calculated from Brunauer-Emmett-Teller (BET) equation by using the $P/P_o = 0.3–0.1$ data of the N_2 adsorption isotherm is 116 m^2/g. Although micropores and disordered mesopores caused by the partially amorphous nature of the natural zeolite support material (deAl-CLI: 147 m^2/g) were occupied by TiO_2 crystals which resulted with a decrease in the BET surface area, the zeolitic support preserved its porous crystalline structure which couldn't be detected by XRD.

EDX analysis seen in Fig. S1 has the signals of K_α values; Al (1.486 keV), Si (1.739 keV), K (3.312 keV) and Ca (3.690 keV) which is from CLI and also Ti (4.508 keV). In this spectrum, there is no Cl element signal which is from the hydrothermal loading of $TiCl_4$ in weak acidic medium has disappeared because of the oxidation reactions appeared during calcination at 700 °C [26]. In addition, it is found out that there are still non-oxidized Ti-Cl groups in products which were obtained with calcination at 600 °C or under, whereas in XRD diffractograms, the d-spacing values for the product calcined at 600 °C fits better with TiO_2 crystal (Fig. 1). In this sample, because there are amorphous groups that contains Cl atoms within a crystal phase, it is expected that the crystalline order increases as Cl atoms leaves as HCl when oxidation process occurs. Although all the Cl-containing phases disappeared, this small distortion in crystalline TiO_2 diffractions in consequence of the chemical interaction of TiO_2 crystals with the support material. As the crystal growth proceeds with the reaction of Cl atoms and the surface hydroxyl groups of CLI, crystal phase increases with the particle amount interacting with the surface and this condition affects the direction of the crystal growth and crystal particle size. The decrease observed in the crystal size with the reduction of the Cl-containing phase can be interpreted by the condensation of TiO_2 catalyst layer, forming more Ti-O-T (T=Si,Al) groups and getting thinner. In Fig. S1(c), SEM images of the catalyst deAl-CLI-Ti-700 is given. From the enlarged image, it is clearly seen that TiO_2 crystals densely cover the surface of the support.

Thermal stability of deAl-CLI-TiO_2 catalyst was investigated with TGA and DTA analyzes (Fig. 2). In TGA curve, at 30–200 °C, the loss is from the physisorbed water, but in 200–400 °C, it is from the strongly adsorbed water and other volatile compounds. The loss at 400–600 °C is from the condensation of the surface hydroxyl groups. From the DTA curve, there is an endothermic region formed between 200–400 °C, resulting from the desorption of the strongly adsorbed water molecules. The total weight loss of the material was only 4%, indicating that a high thermally stable material was obtained. deAl-CLI-Ti-700 product has neither endothermic nor exothermic transformation observed upon 900 °C.

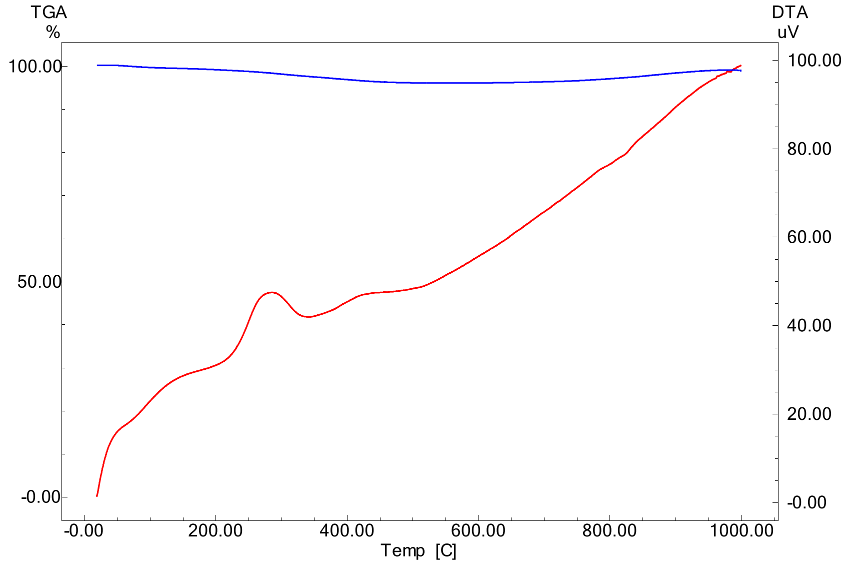

Fig. 2 TGA (blue) and DTA (red) thermograms of deAl-CLI-Ti-700

3.1 Catalytic Tests - Esterification of Octanol with Acetic Acid

The proposed catalytic reaction mechanism is given in Fig. 3. In the reaction medium, firstly acetic acid is interacted with the surface hydroxyl groups of the catalyst with intermolecular forces (H-bonding), then the alcohol reacts with the adsorbed acid molecule to form the alkyl acetate product with condensation. The reaction was monitored by using GC-MS analysis: the reactant, octanol, has (m/z = 130) and the product, octyl acetate, has (m/z = 172), that were consistent with the NIST Mass Spec Data library.

3.1.1 The Effect of Reaction Temperature

It is found out that the yield of the esterification is directly related with the change in temperature. The catalytic tests were conducted by using 1 ml octanol, 1.5 ml acetic acid, and 0.1 g catalyst for 3 h. At 100 °C, it can be said that the lack of activation energy resulted with a very low yield. When the temperature was increased to 120 °C, the

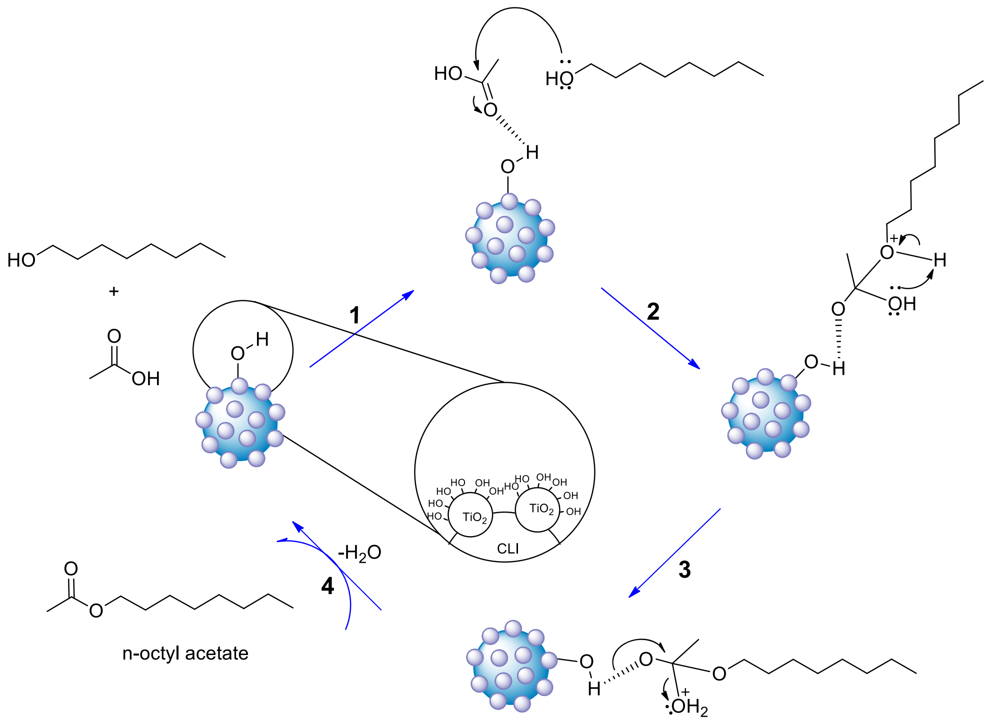

Fig. 3 Proposed catalytic reaction mechanism

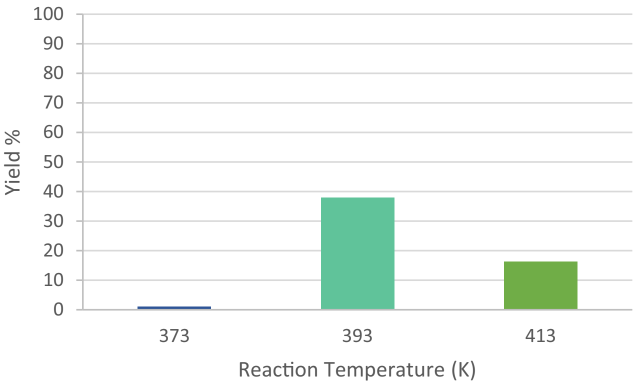

Fig. 4 The yield of the esterification reaction with the change in temperature

reaction yielded 38%, and when increased to 140 °C, the yield decreased to 16.4%. Therefore, the optimum reaction temperature for this reaction is found to be 120 °C (Fig. 4).

3.1.2 The Effect of Reaction Time

The catalytic tests were conducted by using 1 ml octanol, 1.5 ml acetic acid and 0.1 g catalyst at the optimum reaction temperature (120 °C). At different times of the reaction, samples were taken from the reaction medium. At the end of 90 min, the reaction yield is found to be 38%, but after 180 min the reaction is said to be in equilibrium with a yield of 79.5%, as after 360 min the reaction yield was only 81%. For this reason, it can be said that the optimum reaction time is 180 min (Fig. 5).

3.1.3 The Effect of Catalyst/Reactant Ratio

The tests were conducted by using 1 ml octanol, 1.5 ml acetic acid, and different amounts of catalysts at 120 °C for 180 min. The maximum yield was obtained with a 0.15 g catalyst/1 ml octanol ratio (Fig. 6). The optimum catalyst/reactant ratio is necessary in order to obtain the most efficient catalyst performance for this reaction. As for the ratio 0.15 g catalyst/1 ml octanol, the active sites on the catalyst is the most suitable for the alcohol and acid molecules to interact and to react to form the ester compound.

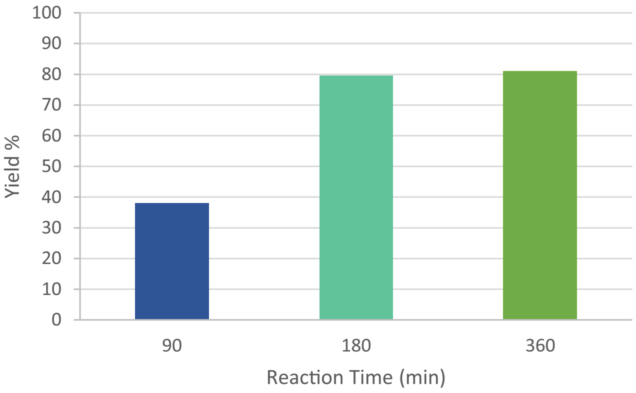

Fig. 5 The change of the esterification reaction yield within time

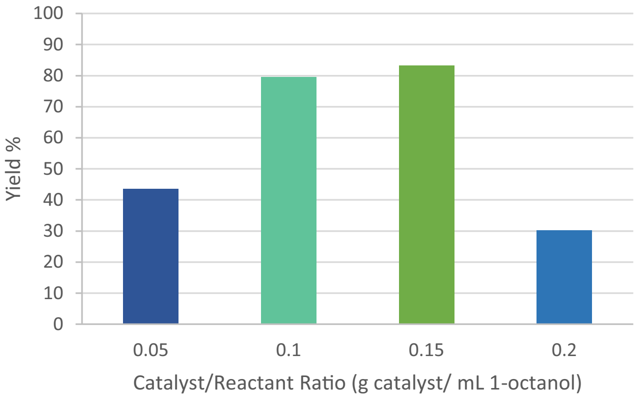

Fig. 6 The effect of catalyst/reactant ratio over the esterification reaction yield

3.1.4 The Reusability of the Catalyst

The reusability tests were conducted at the optimum reaction conditions (120 °C, 180 min, 0.15 g catalyst/1mL octanol ratio). In each cycle, at the end of the reaction, the catalyst was separated from the final mixture by filtration, then washed with distilled water, acetone and dichloromethane in order to remove impurities, then used for the next cycle. At the second cycle, yield was 71.5% with a decrease of only by 13.9% from the first cycle, and at third cycle the yield was 47.8%, decreasing by 33.1%. This shows that the reduction in catalytic activity is due to the reactants or products blocking the active sites on the surface of the catalyst. It can be said that better techniques of regeneration of the catalyst such as calcination or washing with different solvent systems can be used for further studies.

4 Conclusion

Within the scope of this study, clinoptilolite-supported anatase TiO_2 catalyst system was synthesized. The catalytic activity of the clinoptilolite-supported TiO_2 was investigated for the esterification reaction of 1-octanol. In this context, optimum reaction conditions such as temperature, time, and catalyst/reactant ratio were determined and found out that at 120 °C, 180 min, 0.15 g catalyst/1mL octanol ratio is the optimum reaction conditions for this catalytic reaction system. Later, the reusability of the catalyst were tested up to 3 cycles with a moderate loss of catalytic activity.

Acknowledgements This study is financed by Hacettepe University with the projects FHD-2016-12145 and FDS-2016-10347.

References

1. Khoshbin R, Haghighi M, Asari N (2013) Direct synthesis of dimethyl ether on the admixed nanocatalysts of CuO–ZnO–Al_2O_3 and HNO_3-modified clinoptilolite at high pressures: surface properties and catalytic performance. Mater Res Bull 48:767–777
2. Asgari N, Haghighi M, Shafiei S (2013) Synthesis and physicochemical characterization of nanostructured CeO_2/clinoptilolite for catalytic total oxidation of xylene at low temperature. Environ Prog Sustain 32:587–597
3. Yosefi L, Haghghi M, Allahyari S, Ashkriz S (2015) The beneficial use of HCl-activated natural zeolite in ultrasound assisted synthesis of Cu/clinoptilolite–CeO_2 nanocatalyst used for catalytic oxidation of diluted toluene in air at low temperature. J Chem Technol Biotechnol 90:765–774
4. Jamalzadeh Z, Haghighi M, Asgari N (2014) Synthesis and physicochemical characterizations of nanostructured Pd/carbon-clinoptilolite-CeO_2 catalyst for abatement of xylene from waste gas streams at low temperature. J Ind Eng Chem 20:2735–2744
5. Khosbin R, Haghighi M (2013) Preparation and catalytic performance of CuO-ZnO-AlO_3/clinoptilolite nanocatalyst for single-step synthesis of dimethyl ether from syngas as a green fuel. J Nanosci Nanotechnol 13:4996–5003
6. Shankar MV, Anandan S, Venkatachalam N, Arabindoo B, Murugesan V (2006) Fine route for an efficient removal of 2,4-dichlorophenoxyacetic acid (2,4-D) by zeolite-supported TiO_2. Chemosphere 63:1014–1021
7. Nikazar M, Gholivand K, Mahanpoor K (2008) Photocatalytic degradation of azo dye Acid Red 114 in water with TiO_2 supported on clinoptilolite as a catalyst. Desalination 219:293–300
8. Yamashita H, Kawasaki S, Yuan S, Maekawa K, Anpo M, Matsumura M (2007) Efficient adsorption and photocatalytic degradation of organic pollutants diluted in water using the fluoride-modified hydrophobic titanium oxide photocatalysts: Ti-containing Beta zeolite and TiO_2 loaded on HMS mesoporous silica. Catal Today 126:375–381
9. Zabihi-Mobarakeh H, Nezamzadeh-Ejhieh A (2015) Application of supported TiO_2 onto Iranian clinoptilolite nanoparticles in the photodegradation of mixture of aniline and 2, 4-dinitroaniline aqueous solution. J Ind Eng Chem 26:315–321
10. Raitu C, Monea F, Lazau C, Grozescu I, Radovan C, Schooman J (2010) Electrochemical oxidation of p-aminophenol from water with boron-doped diamond anodes and assisted photocatalytically by TiO_2-supported zeolite. Desalination 260:51–56
11. Kajaju DK, Kockler J, Motti CA, Glass BA, Oelgemöller M (2015) Titanium dioxide/zeolite integrated photocatalytic adsorbents for the degradation of amoxicillin. Appl Catal B: Environ 166–167:45–55
12. Rahmani F, Haghighi M, Vafaeian Y, Estifaee P (2014) Hydrogen production via CO_2 reforming of methane over ZrO_2-Doped Ni/ZSM-5 nanostructured catalyst prepared by ultrasound assisted sequential impregnation method. J Power Sources 272:816–827
13. Kajeh Talkhoncheh S, Haghighi M (2015) Syngas production via dry reforming of methane over Ni-based nanocatalyst over various supports of clinoptilolite, ceria and alumina. J Nat Gas Sci Eng 23:16–25
14. Yu Y, Wang J, Parr JF (2012) Preparation and properties of TiO_2/fumed silica composite photocatalytic materials. Procedia Eng 27:448–456
15. Arconada N, Duran A, Suarez S, Portela R, Coronado JM, Sanchez B, Castro Y (2009) Synthesis and photocatalytic properties of dense and porous TiO_2-anatase thin films prepared by sol–gel. Appl Cat B: Environ 86:1–7
16. Vernardou D, Strarakis E, Kenanakis G, Yates HM, Couris S, Pemble ME, Koudomas E, Katsarakis N (2009) One pot direct hydrothermal growth of photoactive TiO_2 films on glass. J Photoch Photobio A 202:81–85
17. Tian H, Ma J, Li K, Li J (2008) Photocatalytic degradation of methyl orange with W-doped TiO_2 synthesized by a hydrothermal method. Mater Chem Phys 112:47–51
18. Chakraborti AK, Singh B, Chankeshwara SV, Patel AR (2009) Protic acid immobilized on solid support as an extremely efficient recyclable catalyst system for a direct and atom economical esterification of carboxylic acids with alcohols. J Org Chem 74:5967–5974
19. Balakrishnan T, Rajendran V (2000) Polymer supported reagents. III. Kinetic study of synthesizing n-octylacetate using insoluble titanium tetrachloride. J Appl Polym Sci 78:2075–2080
20. Choudary BM, Bhaskar V, Kantam ML, Rao KK, Raghavan KV (2002) Process for the production of esters from alcohols using acetic acid as acetylating and clays as catalysts. US Patent 6472555
21. Izumi Y, Hisano K, Hida T (1999) Acid catalysis of silica-included heteropolyacid in polar reaction media. Appl Cat A: Gen 181:277–282
22. Akyalçın S, Altıokka MR (2012) Kinetics of esterification of acetic acid with 1-octanol in the presence of Amberlyst 36. Appl Cat A: Gen 429–430:79–84
23. Khder AERS, Hassan HMA, El-Shall MS (2012) Acid catalyzed organic transformations by heteropoly tungstophosphoric acid supported on MCM-41. Appl Cat A: Gen 411–412:77–86
24. Howard CJ, Sabine TM, Dickson F (1992) Structural and thermal parameters for rutile and anatase. Acta Cryst 47:462–468
25. Zuruzi AS, Kolmakov A, MacDonald NC, Moskovits M (2006) Highly sensitive gas sensor based on integrated nanosponge arrays. Appl Phys Lett 88:102904-102904-3
26. Enriquez J, Lajas L, Alamilla R, Martin E, Alamilla P, Handy E, Galindo G, Serrano L (2013) Synthesis of solid acid catalysis based on TiO_2-SO_4^{2-} and Pt/ TiO_2-SO_4^{2-} applied in n-hexane isomerization. Open J Metal 3:34–44